Available online at www.sciencedirect.com
ScienceDirect
Journal of the European Ceramic Society 30 (2010) 2563–2567
www.elsevier.com/locate/jeurceramsoc

3D printing of bone substitute implants using calcium phosphate and bioactive glasses

Christian Bergmann [a,*], Markus Lindner [a], Wen Zhang [b], Karolina Koczur [a], Armin Kirsten [a], Rainer Telle [b], Horst Fischer [a]

[a] Department of Dental Materials and Biomaterials Research, University Hospital Aachen, Pauwelsstrasse 30, D-52074 Aachen, Germany
[b] Department of Ceramics and Refractory Materials, RWTH Aachen University, Mauerstrasse 5, D-52064 Aachen, Germany

Received 3 November 2009; received in revised form 24 March 2010; accepted 26 April 2010
Available online 23 May 2010

Abstract

Customized implants for bone replacement are a great help for a surgeon to remodel maxillofacial or craniofacial defects in an esthetical way, and to significantly reduce operation times. The hypothesis of this study was that a composite of β-tricalcium phosphate (β-TCP) and a bioactive glass similar to the 45S5 Henchglass® is suitable to manufacture customized implants via 3D-printing process. The composite was chosen because of the bioresorption properties of the β-TCP, its capability to react as bone cement, and because of the adjustability of the bioactive glass from inert to bioresorbable. Customized implants were manufactured using the 3D-printing technique. The four point bending strength of the printed specimens was 14.9 MPa after sintering. XRD analysis revealed the occurrence of two other phases, $CaNaPO_4$ and $CaSiO_3$, both biocompatible and with the potential of biodegradation. We conclude that it is possible to print tailored bone substitute implants using a bioactive TCP/glass composite. The glass is not involved as reactive substance in the printing process. This offers the opportunity to alter the glass composition and therefore to vary the composition of the implant.

Keywords: 3D printing; β-Tricalcium phosphate; Bone substitute; Biodegradation; Bioactive glass

1. Introduction

The "golden standard" for treating small bone defects is autologous bone (bone derived from the same patient). It has excellent bioresorption capabilities and is never rejected by the body.[1] However, large-scale defects are difficult to restore this way, because the extraction of large amounts of autologous tissue can cause donor side problems, like morbidity or iliac wing fractures.[2–4] For those defects solid implants consisting of synthetic materials have to be manufactured, which reconstruct the bone and support it mechanically. Calcium phosphates are widely used as bone substitute materials.[5–7] Especially β-tricalcium phosphate (β-TCP) is known for its good bioresorption properties.[8–10] β-TCP can react with phosphoric acid as bone cement, forming dicalcium hydrogen phosphate (DCPD) and dicalcium pyrophosphate (DCPP), which are also bioresorbable calcium phosphates.[11–13] Biocompatible glasses, on the other side, can be adjusted from bioinert to bioresorbable according to their composition.[14,15] Both materials, in form of granules or pastes, are already in clinical application.

The hypothesis of this study was that a combination of β-TCP and biocompatible glass is advantageous for the manufacturing of bone implants with a 3D-printing technique. 3D printing is a rapid manufacturing method, were a binding solution is printed into layers of powder, accordingly to a sliced virtual model. This method is already in the focus of scientific research for customized scaffolds.[16,17] In this study the focus was to investigate, if the different properties of β-TCP and biocompatible glass could prove advantage for the 3D printing of customized, bioresorbable, large-scale bone implants.

2. Experimental

2.1. Preparation of granulate

β-TCP was synthesized, by heating calcium deficient hydroxyapatite ($Ca_3(PO_4)_2$ art. no. 1.02143.9026 Merck Darmstadt, FRG) for 1 h at 1000 °C. Beforehand exact calcium to

* Corresponding author. Tel.: +49 241 8080936; fax: +49 241 8082027.
E-mail address: chbergmann@ukaachen.de (C. Bergmann).

0955-2219/$ – see front matter © 2010 Elsevier Ltd. All rights reserved.
doi:10.1016/j.jeurceramsoc.2010.04.037

phosphorus ratio of 1.5 was adjusted by adding 5 wt.% of calcium hydrogen phosphate dihydrate ($CaHPO_4 \cdot 2H_2O$ art. no. 1.02144.9025 Merck Darmstadt, FRG). After heating, the mixture was analyzed using XRD.

Bioactive glass similar to 45S5 Henchglass®, further referred to as BGH glass, was synthesized using 33.67 g of silica SiO_2 (SIKRONSH 200, Quarzwerke, Frechen FRG), 31.34 g of sodium carbonate anhydrous (Na_2CO_3 art. no. 6392.5000, Merck, Darmstadt, FRG), 26.38 g calcium carbonate ($CaCO_3$ art. no. 1.02063.5000, Merck, Darmstadt, FRG) and 8.61 g of calcium hydrogen phosphate anhydrous ($CaHPO_4$, art. no. 1.02144.9025, Merck, Darmstadt, FRG). The powders were blended in a dry mixer for 30 min and filled in a platinum crucible. The crucible was placed into a preheated furnace and the powder was melted at 1300 °C for 1 h and 45 min. The hot melt was poured into water. The produced glass frit was dried at 60 °C for 24 h and analyzed by X-ray fluorescence yield and X-ray diffraction technique.

The granules consisting of β-TCP and BGH glass were synthesized via spray drying. First a water based suspension with 40 wt.% of β-TCP and 60 wt.% of BGH glass was prepared and milled in a ball mill. The milled suspension was granulated at 230 °C using a spray dryer (Mobile minor 2000, Niro, Soeborg, Denmark) and the size distribution of the obtained granulate was analyzed by a laser granulometer.

2.2. 3D-printing tests

The granulate was used as powder in a 3D-printing device (Designmate CX, Z-Corporation, Burlington, USA). For the 3D-printing tests the binding solution, the layer thickness, the saturation, and the geometry in the building chamber was investigated. Different combinations of orthophosphoric acid (H_3PO_4 art. no. 30417, Sigma–Aldrich, Seelze, FRG) and pyrophosphoric acid ($H_7P_2O_7$ art. no. 60352, Sigma–Aldrich, Seelze, FRG), varying between 0 and 1.5 mol, in combination with isopropanol were tested as printing solutions. The phosphoric acids were dissolved in distilled water and mixed with isopropanol as necessary. The solutions were filled into the printing heads of the 3D-printer device and printed into the powder bed. The amount of solution printed per mm^3 granulate was varied between 0.376 and 0.94 ml. Structures with different thicknesses of the layers were built up. The thickness of the applied powder layers was varied between 25 and 100 μm. The printed structures were taken out of the powder bed and cleaned using oil free compressed air supplied in-house from the university hospital. The samples were post processed at 1000 °C to increase the mechanical strength. The temperature of 1000 °C was chosen to avoid the forming of α-TCP, which starts at 1125 °C.

2.3. Mechanical tests

The mechanical tests were performed on specimens with rectangular cross section (6 mm × 8 mm × 45 mm). The characteristic strength σ_0 was determined in a four point bending test. The inner and outer roller spans were 20 and 40 mm. The cross-head speed during loading in the universal testing machine (Z030, Zwick, Ulm, FRG) was 5 mm/min. Ten specimens that were heat treated at 1000 °C were tested.

Table 1
Phase composition of the synthesized BGH glass in comparison to the theoretical composition of 45S5 Henchglass®.

Component	45S5 Henchglass® theoretical	BGH glass
SiO_2	45.00 wt.%	45.35 ± 0.01 wt.%
Al_2O_3	0.00 wt.%	0.14 ± 0.01 wt.%
TiO_2	0.00 wt.%	0.02 ± 0.01 wt.%
CaO	24.50 wt.%	24.92 ± 0.01 wt.%
Na_2O	24.50 wt.%	23.10 ± 0.01 wt.%
P_2O_5	6.00 wt.%	6.21 ± 0.01 wt.%

2.4. Generation of a 3D implant model

A virtual 3D model of an implant was derived from a computer tomography data set. The model was converted into a stl-file (**s**urface **t**esselation **l**anguage) which is a standard software interface for rapid manufacturing devices. The model was printed with the 3D printer and heat treated at 1000 °C.

3. Results

The XRD analysis of the synthesized calcium phosphate showed a pure β-TCP phase. Hydroxyapatite, which forms when the Ca/P ratio is higher than 1.5, was not detected. The accuracy of the XRD analysis of β-TCP in respect of the HA content is less than 1%. The synthesized BGH glass was also analyzed using XRD and its element composition was determined using X-ray fluorescence yield. The XRD diagram did not reveal any peaks of crystallized material, only an intensity increase between $2\theta = 28°$ and $2\theta = 35°$, which is typical for the short range order of glass phases. The X-ray fluorescence yield showed a phase composition close to the theoretical composition of 45S5 Henchglass® (Table 1). The spray dried granules of 60 wt.% BGH glass and 40 wt.% β-TCP had a grain size distribution of $d_{10} = 18$ μm, $d_{50} = 41$ μm and $d_{90} = 92$ μm. The grains consisted out of a homogeneous mixture of BGH glass and β-TCP (Fig. 1).

Printing solutions with concentrations of phosphoric acid lower than 2 mol/l were not suitable for binding the printed structures with high enough strength to get them safely out of the powder bed. Concentrations of phosphoric acid with 2 or more mol/l were only printable with the addition of 20 wt.% of isopropanol. Without isopropanol the print heads overheated and the process became instable. Therefore the best solution for the printing process was the combination of 1 mol/l of orthophosphoric acid and 1 mol/l of pyrophosphoric acid with 20 wt.% of isopropanol. The printed structures could be easily taken out of the powder bed and cleaned with compressive air. 0.414 ml of binding solution per mm^3 granulate was ideal for a detailed profile of the printed structures in combination with sufficient mechanical strength for cleaning the structures with compressive air. Higher amounts of solution per mm^3 granulate degraded the profile accuracy.

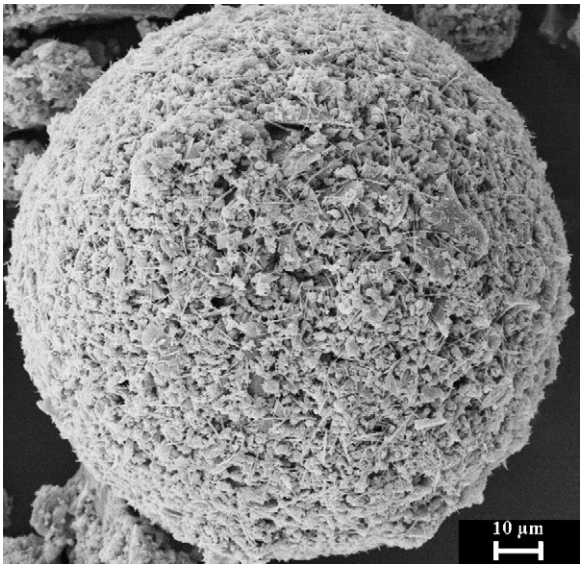

Fig. 1. SEM micrograph of a 60 wt.% BGH glass and 40 wt.% β-TCP granule. Both components are distributed homogeneously.

The layer thickness had also a high influence on the mechanical strength of the printed structures. With a thickness of 87.5 μm or higher only very brittle structures were producible. Single layers easily broke under shear stresses. On the other hand a too small layer thickness of 35 μm or lower caused direct sheering of the layers during the printing process. The best printing results were achieved using a layer thickness between 50 and 75 μm.

The mechanical properties were significantly increased by the heat treatment of the printed structures. The bending strength of the specimens treated at 1000 °C was 14.9 ± 3.6 MPa. The heat treatment changed the phase composition of the printed structures. Fig. 2 shows the XRD diagrams of the specimens before and after the heat treatment. The β-TCP phase which is the only dominant phase in the non-treated sample disappeared and was replaced by a phase mixture of $NaCaPO_4$ and $CaSiO_3$.

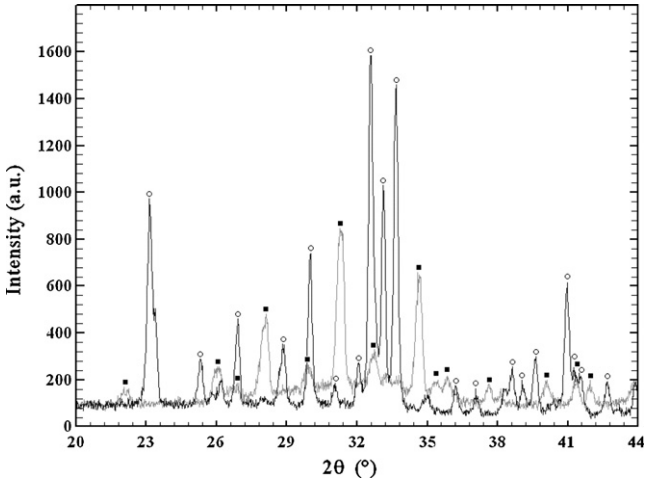

Fig. 2. XRD diagrams of an untreated (grey line marked with black squares) and at 1050 °C heat treated (black line marked with white circles) printed structure. After the heat treatment, the β-TCP phase disappeared and new phases ($NaCaPO_4$ and $CaSiO_3$) occurred.

4. Discussion

The calcium to phosphorus ratio of hydroxyapatite (HA) is 10% higher than that of β-TCP (β-TCP Ca/P = 1.5, HA Ca/P = 1.67). One may assume that 1% of HA will form as a second phase during the synthesis of β-TCP, when there is 0.1% more calcium in the mixture than needed for the exact Ca/P ratio of β-TCP. If the ratio is lower than 1.5 calcium pyrophosphate (CPP) (Ca/P = 1) will be formed as a second phase. In this case 0.3% of CPP will form, if there is 0.1% less calcium in the starting mixture than needed for the synthesis of β-TCP. The missing main peak of HA at $2\theta = 31.73^\circ$ (ICDD no. 24-33) in the XRD diagram indicates a phase purity of the β-TCP with an error of less than 1%, as Peters et al. already described elsewhere.[18]

The BGH glass was synthesized with a composition similar, but not exactly as the theoretical composition of the 45S5 Henchglass®. Yet the BGH glass is still within the composition range of a bioactive glass, as described by different researchers.[14,19,20] As found by the researchers the glass can be bond to both, hard and soft tissue.

The size distribution and round shape of the spray dried granulates were suitable for producing plain and flawless powder layers during the 3D-printing process. The granules had also a homogeneous distribution of the two components β-TCP and BGH glass, which is important for a reliable binding reaction during the printing process and homogeneous properties of the fabricated implant.

For the optimization of the 3D-printing parameters not only the mechanical strength of the build-up structure had to be taken into account, but also the profile and the bonding between each layer. Higher amounts of acid solution printed into the powder bed caused an intensification of the binding reaction, but deteriorated the profile of the 3D structures. A too thin or too thick layer thickness influenced the bonding between the powder layers, resulting in shearing of the layers during or after the printing process. The best parameters found for the printing of structures using a granulate consisting of β-TCP with BGH glass were a layer thickness between 50 and 75 μm, a concentration of the binding solution of 1 mol/l orthophosphoric acid, 1 mol/l of pyrophosphoric acid and 20 wt.% of isopropanol, and 0.414 ml of solution printed per 1 mm^3 β-TCP granulate. With these parameters the reconstruction of an implant derived from CT data was printed (Fig. 3).

The heat treatment of the β-TCP, BGH glass mixture increased the four point bending strength two times higher than a post treatment of printed structures consisting of pure calcium phosphates.[21–23] Nevertheless the bending strength of approximately 15 MPa is still 10 times lower than that of natural bone.[24]

Reactions between the β-TCP, the DCPD and the bioactive glass during the heat treatment of the printed structures, generated the phases $CaNaPO_4$ and $CaSiO_3$. Those two phases are both bioactive with the potential of biodegradation depending on the phase composition and the porosity of the implant.[25–30] Respecting the printing process of the structures, the glassy phase of the granules has no effect on the cement reaction. Therefore the glass content can be varied to generate tailored

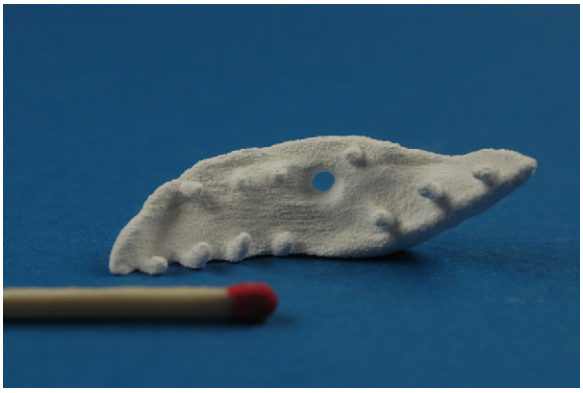

Fig. 3. Printed structure of a model of an implant generated from CT data. The implant was printed with a commercial 3D printer using granulate consisting of β-TCP and BGH glass.

biodegradation capabilities of the implant after the treatment process.

5. Conclusion

The study confirmed that a composite material made of β-TCP and a bioactive glass is suitable for the build-up of 3D printed structures. The samples were printed with a maximum resolution of 50 μm according to the smallest applied layers. Structures generated from computer tomography data, displaying implants for real applications, were producible. Although the phase composition changed to wollastonite ($CaSiO_3$) and rhenanite ($CaNaPO_4$) after the post process at 1000 °C the biocompatibility should still be given as proved by others.[25–30] Only the β-TCP phase was necessary for the printing process, while the glass phase had no influence. Therefore the adjustability of the glass composition holds the possibility for tailored biodegradation kinetics in an in vivo application.

The disadvantage of customized, 3D-printed implants is the high production costs for a limited number of cases. Also a partially degradation of synthetic implants is not a priori advantage for the patient in every case, because remaining fragments can weaken the mechanical strength of the new grown bone. In further developments the degradation behavior of the implants has to be improved by optimizing the phase composition and porosity. The formation of new tissue should also be stimulated by the addition of growth factors or other pharmaceuticals.

Acknowledgement

The authors want to acknowledge Dr. Arno Kaiser, Institute of Mineral Engineering, RWTH Aachen University, for his support with the characterisation of BGH glass.

References

1. Infante-Cossio P, Gutierrez-Perez JL, Torres-Lagares D, Garcia-Perla Garcia A, Gonzalez-Padilla JD. Bone cavity augmentation in maxillofacial surgery using autologous material. *Rev Esp Cir Oral Maxillofac* 2007;**29**:7–19.
2. Vail TV, Urbaniak JR. Donor-site morbidity with use of vascularized autogenous fibular. *J Bone Joint Surg Am* 1996;**78**:204–11.
3. Bloemers FW, Blokhuis TJ, Patka P, Bakker FC, Wippermann BW, Haarman HJTM. Autologous bone versus calcium-phosphate ceramics in treatment of experimental bone defects. *J Biomed Mater Res B* 2003;**66B**:526–31.
4. Arrington ED, Smith WJ, Chambers HG, Bucknell AL, Davino NA. Complications of iliac crest bone graft harvesting. *Clin Orthop Relat R* 1996;**329**:300–9.
5. Frayssinet P, Mathon D, Lerch A, Autefage A, Collard P, Rouquet N. Osseointegration of composite calcium phosphate bioceramics. *J Biomed Mater Res* 2000;**50**:125–30.
6. Webster TJ, Siegel RW, Bizios R. Enhanced functions of osteoblasts on nanophase ceramics. *Biomaterials* 2000;**21**:1803–10.
7. Murugan R. Bioresorbable composite bone paste using polysaccharide based nano hydroxyapatite. *Biomaterials* 2004;**25**:3829–35.
8. von Doernberg MC, von Rechenberg B, Bohner M, Grünenfelder S, van Lenthe GH, Müller R, et al. In vivo behavior of calcium phosphate scaffolds with four different pore sizes. *Biomaterials* 2006;**27**:5186–98.
9. Klein CPAT, Driessen AA, de Groot K. Biodegration behavior of various calcium phosphate materials in bone tissue. *J Biomed Mater Res* 1983;**17**:769–84.
10. Hoshino M, Egi T, Terai H, Namikawa T, Takaoka K. Repair of long intercalated rib defects using porous beta-tricalcium phosphate cylinders containing recombinant human bone morphogenetic protein-2 in dogs. *Biomaterials* 2006;**27**:4934–40.
11. Theiss F, Apelt D, Brand B, Kutter A, Zlinszky K, Bohner M, et al. Biocompatibility and resorption of a brushite calcium phosphate cement. *Biomaterials* 2005;**26**:4383–94.
12. Apelt D, Theiss F, El-Warrak AO, Zlinszky K, Bettschart-Wolfisberger R, Bohner M, et al. In vivo behavior of three different injectable hydraulic calcium phosphate cements. *Biomaterials* 2004;**25**:1439–51.
13. Grover ML, Gbureck U, Wright AJ, Tremayne M, Barralet JE. Biological mediated resorption of brushite cement in vitro. *Biomaterials* 2006;**27**:2178–85.
14. Hench LL. Ceramic implants for humans. *Adv Ceram Mater* 1986;**1**:306–24.
15. Hench LL. The story of Bioglass®. *J Mater Sci: Mater Med* 2006;**17**:967–78.
16. Seitz H, Rieder W, Irsen S, Leukers B, Tille C. Three-dimensional printing of pourous ceramic scaffolds for bone tissue engineering. *J Biomed Mater Res Part B: Appl Biomater* 2005;**74B**:782–8.
17. Fierz FC, Beckmann F, Huser M, Irsen SH, Leukers B, Witte F, et al. The morphology of anisotropic 3D-printed hydroxyapatite scaffolds. *Biomaterials* 2008;**29**:3799–806.
18. Peters F, Reif D. Functional materials for bone regeneration from beta-tricalcium phosphate. *Mat -wiss u Werkstofftech* 2004;**35**: 203–7.
19. Andersson ÖH, Liu G, Kangasniemi K, Juhanoja J. Evaluation of the acceptance of glass in bone. *J Mater Sci: Mater Med* 1992;**3**: 145–50.
20. Kokubo T. Bioactive glass ceramics: properties and applications. *Biomaterials* 1991;**12**:155–63.
21. Gbureck U, Hölzel T, Klammert U, Würzler K, Müller FA, Barrale JE. Resorbable dicalcium phosphate bone substitutes prepared by 3D powder printing. *Adv Funct Mater* 2007;**17**:3940–5.
22. Gbureck U, Hölzel T, Biermann I, Barralet JE, Grover LM. Preparation of tricalcium phosphate/calcium pyrophosphate structures via rapid prototyping. *J Mater Sci: Mater Med* 2008;**19**:1559–63.
23. Müller B, Deyhle H, Fierz FC, Irsen SH, Yoon JY, Mushkolaj S, et al. Bio-mimetic hollow scaffolds for long bone replacement. *Proc SPIE* 2009;**7401**:74010D–1D.
24. Reilly DT, Burstein AH. The mechanical properties of cortical bone. *J Bone Joint Surg Am* 1974;**56**:1001–22.
25. Knabe C, Berger G, Gildenhaar R, Howlett CR, Markovic B, Zreiqat H. The functional expression of human bone-derived cells grown on rapidly resorbable calcium phosphate ceramics. *Biomaterials* 2004;**25**: 335–44.

26. Ramselaar MMA, Van Mullem PJ, Kalk W, Driessens FCM, De Wijn JR, Stols ALH. In vivo reactions to particulate rhenanite and particulate hydroxylapatite after implantation in tooth sockets. *J Mater Sci: Mater Med* 1993;**4**:311–7.
27. Driessens FCM, Ramselaar MMA, Schaeken HG, Stols ALH, Van Mullem PJ, De Wijn JR. Chemical reactions of calcium phosphate implants after implantation in vivo. *J Mater Sci: Mater Med* 1992;**3**: 413–7.
28. Jalota S, Bhaduri SB, Tas AC. A new rhenanite (β-$NaCaPO_4$) and hydroxyapatite biphasic biomaterial for skeletal repair. *Mater Res Part B: Appl Biomater* 2007;**80B**:304–16.
29. Teramoto H, Kawai A, Sugihara S, Yoshida A, Inoue H. Resorption of apatite-wollastonite containing glass-ceramic and beta-tricalcium phosphate in vivo. *Acta Med Okayama* 2005;**59**:201–7.
30. Wue W, Liu X, Zheng XB, Ding C. In vivo evaluation of plasma sprayed wollastonite coating. *Biomaterials* 2005;**26**:3455–60.